IR Spectra of Photopolymerized C_{60} Films. Experimental and Density Functional Theory Study

Stepan G. Stepanian,[†] Victor A. Karachevtsev,[†] Alexander M. Plokhotnichenko,[†] Ludwik Adamowicz,*[,‡] and Apparao M. Rao[§]

Institute for Low-Temperature Physics and Engineering, NAS of Ukraine, Kharkov, 61103, Ukraine, Department of Chemistry, University of Arizona, Tucson, Arizona 85721, and Department of Physics and Astronomy, Clemson University, Clemson, South Carolina 29634-0978

Received: July 13, 2005; In Final Form: May 21, 2006

IR spectra of photopolymerized fullerene films obtained by simultaneous deposition and UV irradiation were measured in the range of 1500−450 cm^{-1}. The degree of the polymerization of the C_{60} films was estimated to be about 95%. To assist the assignment of the experimental IR spectra of the films, quantum chemical calculations of the equilibrium structures of the C_{60} dimers and trimers were performed at the DFT(B3LYP)/3-21G level of theory. Next, IR frequencies and intensities for those structures were calculated. For the five-trimer structures found in the calculations, the relative stabilities were determined at the B3LYP/4-31G* and B3LYP/6-31G* levels and used to select the lowest-energy trimers, which are Trimer A (angle between monomer centers is 90°) and Trimer B (angle between monomer centers is 120°). Next, the IR spectra of the polymerized fullerene films were compared with the calculated frequencies of the lowest-energy dimer and the two lowest-energy trimers. On the basis of this analysis and on the comparison of the film spectra with the IR spectra of the C_{60} dimer and trimer spectra obtained by other methods, it was shown that the main components of the films are C_{60} dimers and the orthorhombic (O) polymer phase. The tetragonal (T) and rhombohedral (R) polymers, as well as small amounts of monomers, were also found. Although vibrational frequencies of different C_{60} phases are similar in most cases, we found several unique spectral features of the C_{60} dimer and other polymers that may be used to determine the composition of the polymerized C_{60} film.

1. Introduction

Fullerene polymers have attracted considerable scientific interest because of their rich structures and unique properties, as well their wide range of possible technological applications.[1−3] Polymerization of C_{60} occurs as a result of the exposure of thin C_{60} films to visible or ultraviolet (UV) radiation,[4] as well as a result of high pressure and high temperature imposed on bulk C_{60} samples (the HPHT method).[5−9] In the polymerization process, the C_{60} molecules form linear chains and four- or six-membered rings connected by covalent links across the hexagonal faces through the [2,2] cycloaddition reaction.[4] Polymerized C_{60} comprises one-dimensional orthorhombic (O), two-dimensional tetragonal (T), and two-dimensional rhombohedral (R)[5−8] phases. A polymerized fullerene sample typically includes one or more phases, depending on the external factors involved in the polymer formation. It is also possible to obtain single-phased polymerized samples by the HPHT method by varying the external conditions.[3,5,8−11]

Photopolymerization of fullerite by UV irradiation[4,12−25] may have some interesting technological applications related to the production of extended polymeric carbon films. However, the use of one-sided sample irradiation in the polymerization process has a significant disadvantage because it usually results in the formation of highly irregular polymers and polymeric fullerene phases across the depth of the film. Recently, it was shown that this difficulty can be overcome, and a much more uniform film polymerization can be achieved by using an approach involving simultaneous deposition and UV irradiation.[25] The detailed composition of the fullerene photopolymerized film is not yet fully understood. It is believed that, in the first phase of the photopolymerization process, dimers are formed, and this is followed by the formation of trimers and larger clusters.

In this work, we use IR spectroscopy in combination with quantum chemical calculations of the IR vibrational frequencies and intensities to determine the composition of the polymerized C_{60} films obtained by the method of simultaneous deposition and UV irradiation. Our aim is to answer the following questions: Is the composition of the film similar to that of the films obtained by other polymerization techniques? Are the spectral features of the different polymer phases distinct? What level of theory is accurate enough to predict, with a reasonable accuracy, the vibrational spectra of the C_{60} dimer and trimers? The answer to the last question is important since, because of the large size of the systems studied, it is not possible to use high-level post-Hartree−Fock (HF) ab initio methods and extended basis sets in the calculation.

The structure and the relative stability of the C_{60} dimers were studied using semiempirical and low-level ab initio methods,[26−31] as well as the DF-TB[32] method. It was determined that the only dimer structure that has lower energy (at the density functional theory (DFT) level of theory) than two isolated monomers is the C_{60} dimer connected by two parallel single C−C bonds. Neither semiempirical[33] nor HF[34] methods have been capable of predicting the correct relative stabilities of the different dimer structures with respect to two isolated monomers. C_{60} trimers

* Corresponding author. E-mail: ludwik@u.arizona.edu.
[†] NAS of Ukraine.
[‡] University of Arizona.
[§] Clemson University.

10.1021/jp053867y CCC: $33.50
Published on Web 07/27/2006

were also studied using semiempirical[33] and HF/3-21G methods.[34] The HF calculations yielded five equilibrium trimer structures, and the cyclic trimer structure was found to have the lowest energy.[34]

2. Calculations

In the first step, the geometries of the C_{60} monomer, four dimers, and five trimers were fully optimized at the DFT level of theory. The DFT calculations were carried out with the three-parameter density functional, usually abbreviated as B3LYP, which includes Becke's gradient exchange correction,[35] the Lee/Yang/Parr correlation functional,[36] and the Vosko, Wilk, and Nusair correlation functional.[37] The standard 3-21G basis set was used. Next, the harmonic IR frequencies and intensities were calculated. Relative stabilities of the five trimers were also determined with the use of the B3LYP/4-31G* and B3LYP/6-31G* levels. Additionally, we performed geometry optimizations and frequency calculations for the C_{60} monomer and the lowest-energy dimer at the B3LYP/4-31G* level. All calculations were performed using the Gaussian 03 program package.[38]

3. Experimental Details

The experimental setup used to produce uniformly photopolymerized fullerene films has been described elsewhere.[25,39] Fullerite powder (purity 99.5 wt %, purchased from the Fullerene Technology Co., St. Petersburg, Russia) was evaporated from a graphite Knudsen cell at temperatures in the 450−500 °C range. The powder sample was degassed before evaporation by maintaining the cell temperature between 150 and 200 °C for 3−4 h in a high vacuum (6×10^{-7} Torr) before the experiment. Evaporation rates ranged between 1 and 5 nm/min during the film deposition. The substrate temperature was monitored with a thermocouple and did not exceed 50 °C during the film deposition. Polymerized C_{60} films were prepared on polished KBr single crystals. The film thickness ($d = 1$ μm) was controlled by a quartz microbalance.

A high-pressure 1000 W Hg lamp was used as the light source for inducing the photopolymerization in the C_{60} films. A special filter was used to eliminate the infrared component of the Hg lamp spectrum and to select the 280−420 nm spectral range. During the experiment, the UV light power of 0.07 W was focused on a stripe with the dimensions $\sim 5 \times 20$ mm. The IR spectra of the C_{60} films deposited/irradiated during 27 h were recorded using the Specord IR 75 (Karl Zeis Jena, Germany, spectral resolution 1−3 cm^{-1}, 4000−400 cm^{-1}) spectrometer.

4. Results and Discussion

4.1. Structure and Relative Stabilities of the C_{60} Dimers and Trimers. *4.1.1. Dimers.* Among the various structures of the C_{60} dimers, only those that have two single C−C bonds connecting the two monomers are stable.[27] These dimers may be formed in [2,2] cycloaddition reactions between the monomers. There are two types of C−C bonds in the C_{60} monomer: the bond between two six-membered rings and the bond between six- and five-membered rings. We denote these bonds as (6) and (5), respectively. Depending on the type of the bonds formed in the cycloaddition, four different C_{60} dimers can be formed. They are Dimer A with a connection between (6) and (6) bonds, Dimer B with a connection between (6) and (5) bonds, and Dimer C and Dimer D with connections between (5) and (5) bonds, as shown in Figure 1.

The geometries of the dimers were fully optimized at the B3LYP/3-21G level of theory, and the resulting structures are shown in Figure 2, and their relative stabilities and the lengths of some selected C−C bonds are presented in Table 1. Clearly, the calculations predict a significant energy gap between the lowest-energy Dimer A and the other dimers. Dimer A is the only dimer whose energy is lower than the doubled energy of a C_{60} monomer. The energy difference between Dimer A and two isolated monomers calculated at the B3LYP/3-21G level is 21.7 kJ mol^{-1}. The higher energy of Dimer B (by approximately 80 kJ mol^{-1}) and of Dimers C and D (by approximately 160 kJ mol^{-1}) with respect to Dimer A is most probably due to a significant lengthening (from 1.607 Å in Dimer A to approximately 1.640 Å in the other dimers) of the C−C bonds in those two dimers (see Table 1). Thus, we concluded that Dimers B, C, and D are not formed during the photopolymerization process, and only Dimer A should be considered in the analysis of the experimental IR spectra.

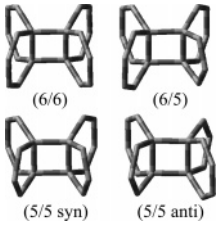

Figure 1. Different types of connections between monomer fragments in the C_{60} dimers.

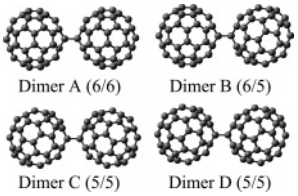

Figure 2. Structures of the C_{60} dimers obtained in the B3LYP/3-21G calculations.

TABLE 1: Relative Stabilities (ΔE, kJ mol^{-1}) and Selected Bond Lengths (Å) of the C_{60} Dimers Calculated at the B3LYP/3-21G Level of Theory[a,b]

			bond length[c]		
	point group	ΔE	C_a-C_a	C_b-C_b	C_a-C_b
Dimer A	D_{2h}	0.0	1.607	1.607	1.590
Dimer B	C_s	82.6	1.607	1.640	1.590
Dimer C	C_{2v}	166.4	1.639	1.639	1.590
Dimer D	C_{2h}	163.6	1.641	1.641	1.590

[a] Relative stabilities are calculated with respect to Dimer A. Its energy is −547.050001 au. [b] Bond lengths of the four-membered ring between the monomer fragments are presented. [c] C_a and C_b are the carbon atoms of the first and second monomer fragments, respectively.

4.1.2. *Trimers.* Since the formation of intermolecular C−C bonds of the (6)/(5) and (5)/(5) types is not possible in the dimers, we limited the consideration of the trimers to only those with (6)/(6) connections. The total number of unique trimer structures with such connections is five. Their structures fully optimized at the B3LYP/3-21G level are shown in Figure 3. Three trimers (Trimers A, B, and C) have bent configurations, and the angles between the centers of the monomers forming those trimers are 90°, 120°, and 145°, respectively. The two other trimers are the linear Trimer D and the cyclic Trimer E. The relative stabilities of the C_{60} trimers calculated at the B3LYP level with the 3-21G, 4-31G* and 6-31G* basis sets are given in Table 2. In all cases, the calculations predict Trimer A to be the lowest energy configuration. Increasing the angle between the monomer centers in the trimer decreases the stability. The

TABLE 2: Relative Stabilities (kJ mol^{-1}) of the C_{60} Trimers Calculated at the Different Levels of Theory for the Geometries Fully Optimized at the B3LYP/3-21G Level

		3-21G			4-31G*		6-31G*	
trimer	point group	HF	B3LYP	MP2	HF	B3LYP	HF	B3LYP
A	C_s	0.0	0.0	0.0	0.0	0.0	0.0	0.0
B	C_1		5.3			3.6		3.2
C	C_1		11.2			10.1		8.5
D	D_{2h}		13.0			11.0		10.8
E	C_{3v}	−17.2	16.0	13.8	15.4	52.7	22.2	55.9

stability order is the same for all three basis sets employed. However, one should note the significant increase in the energy gap between Trimer E and Trimer A and between the other trimers and Trimer A with the increase in the quality of the basis set: from 16.0 (3-21G) to 55.9 kJ mol^{-1} (6-31G*).

The present stability results obtained with the DFT method are different from the results obtained at the HF/3-21G level of theory,[34] which predicted the cyclic trimer to be the most stable. To elucidate the origin of the difference, we performed additional calculations of the relative stabilities of Trimers A and E at the HF level using 3-21G, 4-31G*, and 6-31G* basis sets, as well as at the MP2/3-21G level of theory. The results of the calculations are shown in Table 2. As it is seen, the relative stability of the trimers calculated at the HF level strongly depends on the quality of the basis set. Trimer E is the lowest energy structure only at the HF/3-21G level. Increasing the basis set size decreases the stability of E with respect to A, and, at the HF/4-31G* and HF/6-31G* levels, Trimer E is less stable than Trimer A. This is similar to the DFT results. On the other hand, it is clearly seen that the HF method still overestimates the relative stability of the cyclic Trimer E with respect to Trimer A by approximately 30−35 kJ mol^{-1} compared to the DFT method. The energy difference between Trimers A and E calculated at the MP2/3-21G level is 13.8 kJ mol^{-1} in favor of Trimer A, and this result is in good agreement with the DFT results. This adds credence to the DFT results obtained with the 4-31G* and 6-31G* basis sets. Summarizing, the relative stabilities of the trimers indicate that all trimers except the cyclic Trimer E should be considered in the analysis of the IR spectra of the films.

4.2. Calculated Spectra. It is well-known that only 12 vibrations (four unique triply degenerated frequencies of the T_{1u} symmetry) of the C_{60} monomer are IR active. They are shown in Table 3 together with the results obtained at the

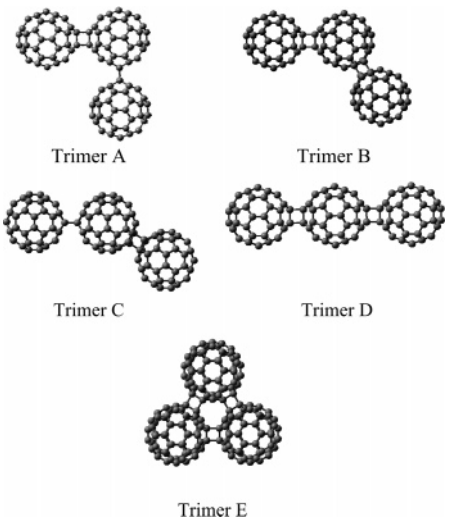

Figure 3. Structures of the C_{60} trimers obtained in the B3LYP/3-21G calculations.

TABLE 3: IR-Active Observed Frequencies and Unscaled Frequencies Calculated at the B3LYP/STO-3G, B3LYP/3-21G, B3LYP/4-31G*, and B3LYP/6-31G* Levels of Theory (ν, cm^{-1}) of the C_{60} Monomer

	calculated							
	STO-3G		3-21G		4-31G*		6-31G*	
observed	ν	Δ	ν	Δ	ν	Δ	ν	Δ
1428	1505	+77	1453	+25	1461	+33	1459	+31
1182	1265	+83	1175	−7	1214	+32	1198	+16
576	595	+19	581	+5	589	+13	587	+11
526	545	+19	506	−20	535	+9	532	+6

B3LYP/STO-3G, B3LYP/3-21G, B3LYP/4-31G*, and B3LYP/6-31G* levels of theory. The comparison of the observed and the predicted frequencies allows us to conclude that the B3LYP/3-21G method is able to produce quite accurate IR frequencies. The average difference between the observed and the unscaled calculated frequencies is less than 15 cm^{-1}. The frequencies calculated with the 3-21G basis set are close to the 4-31G* ones. At the same time, frequencies calculated with the minimal basis set show large deviations from the experimental values. Two frequencies calculated with the 3-21G basis set (1175 and 581 cm^{-1}) are in very good agreement with the experimental values. The deviations are within several reciprocal centimeters. However, the calculations overestimate the higher frequency vibration at 1453 cm^{-1} by 25 cm^{-1} and underestimate the lowest frequency vibration by 20 cm^{-1}. One may expect that the discrepancy between the calculated and the observed frequencies of similar vibrational modes for the dimer and the trimers should be very close to those of the monomer. In such a case, it should be possible to use a uniform scaling factor for calculated frequencies of similar type for the dimer and the trimer to bring them closer to their experimental counterparts. To simplify the procedure, we only used two scaling factors for the C_{60} dimer and trimer frequencies. For the higher frequencies, the scaling factor used was 0.98, and, for the lower frequencies, the factor was 1.04. For other frequencies, we did not apply any scaling. The two scaling factors were determined as ratios between the calculated and the observed frequencies for the monomer.

The C_{60} Dimer A has 120 atoms and, thus, 354 vibrations:

$$46A_g + 44B_{1g} + 44B_{2g} + 42B_{3g} + 44A_u + 44B_{1u} + 44B_{2u} + 46B_{3u}$$

Only the B_{1u}, B_{2u}, and B_{3u} vibrations are IR active. The IR-active dimer and trimer vibrations may be split into three groups: (i) vibrations analogous to the four IR-active monomer vibrations now separated by new intermolecular bonds of the dimer and the trimer; (ii) vibrations that are inactive in the monomer IR spectrum but became active in the spectra of the dimer and the trimer as a result of the decrease of symmetry of those systems in comparison with the monomer; and (iii) vibrations of the fragment connecting the C_{60} monomers. The vibrations of the first group should have frequencies and intensities similar to the monomeric frequencies. The vibrations

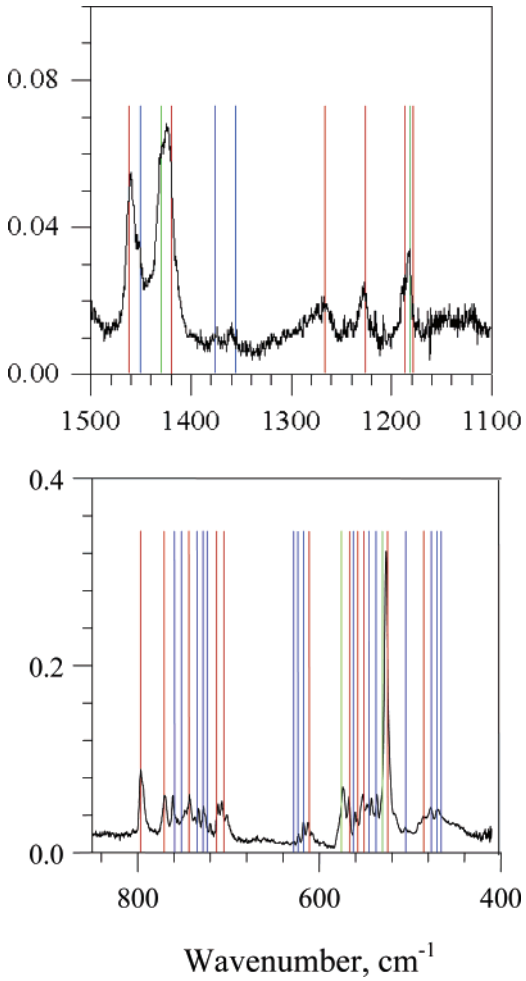

Figure 4. IR spectrum of photopolymerized C_{60} film. Vertical lines correspond to vibrational frequencies calculated at the B3LYP/3-21G level of theory of the monomer (green), of the dimer (red), and the trimers (blue).

of the second group usually have low intensities, and only a few of them are visible in the spectrum.

4.3. Assignment of the IR Spectra of the Irradiated Fullerene Films. In the analysis of the IR spectra of the polymerized films, which is presented in Figure 4, our aim was to identify spectral features that are characteristic to the various fullerene forms that may be present in the film (monomers, dimers, trimers, as well as larger structures). A comparative analysis was carried out for IR absorption spectra of the C_{60} polymers obtained in the present work and of those reported earlier,[4,10,18,40−42] among which there was the spectrum of a photopolymer[4,18] of the C_{60} crystalline film, the spectrum of C_{60} dimers obtained during a solid-state mechanochemical reaction,[40] the spectrum of the C_{60} dimer and a polymer prepared by a solution-based method[42] with photoirradiated fullerene in solution, and the spectrum of a C_{60} polymer obtained by the HPHT method.[10] The solution-based method can only separate the dimer from the polymer; it does not allow one to ascertain the composition of the polymeric phase. The HPHT method permits one to investigate the polymeric fullerene phase; however, the HPHT-generated polymeric fullerene phase may contain contaminations from other phases.

In the following subsections, we describe the assignment of the experimental bands in the different spectral regions. The observed and calculated frequencies are collected in Tables 4−7. In those tables, we also included all active IR frequencies calculated for the C_{60} monomer and some selected active frequencies calculated for the C_{60} dimer and the trimers. We omitted dimer and trimer frequencies with low intensities not observed in IR spectra.

4.3.1. 1500−1300 cm^{-1}. The observed and calculated frequencies in this spectral region are presented in Table 4. In the background of the monomer band at 1428 cm^{-1}, a new band appears at 1422 cm^{-1} that was previously observed for the photopolymer.[4,18] This band may be attributed to either the dimer or the O polymer.[10] The calculations predict a downshift of the monomeric band due to dimerization. The frequency of the monomeric band scaled down by a factor of 0.98 is 1424 cm^{-1}. For the dimer, the calculations predict three active vibrations at 1422, 1421, and 1416 cm^{-1}. Upon polymerization, a rather intense band appears at 1458 cm^{-1} in the spectrum that was also observed for the photopolymer.[4,18] This band is attributed to the calculated dimer frequency of 1460 cm^{-1}. This assignment is confirmed by the assignment made for the dimer spectrum[40] in samples obtained by the HPHT method. A weak band at 1450 cm^{-1} is observed as a shoulder of a higher frequency dimer band, and it may be assigned to the O polymer. This assignment is based on the calculations that predict several bands near the frequency of 1450 cm^{-1} for Trimer D, where the connections between the C_{60} monomers are similar to the connections in the O polymer. The existence of those connections downshifts

TABLE 4: IR Frequencies Observed in the Range of 1500−1300 cm^{-1} (in cm^{-1}) of the Polymerized C_{60} Film and Harmonic Frequencies Calculated at the B3LYP/3-21G Level of Theory of the C_{60} Monomer, Dimer, and Trimers

observed[a]							
this work[b]	ref 18	ref 4	ref 40	ref 42[c]	ref 10[c]	calculated[d]	C_{60} phase[e]
1458 (m)	1460 (m)	1460 (w)	1463 (m)	1458 (m), P	1464 D	1460 (21) Dimer	D
1450 (m)					1446 O	1450 (12) Trimer A	O
						1448 (14) Trimer A	
1428 (m)	1430 (s)			1428 (m), D		1424 (23) Monomer	M
1422 (m)	1424(w)	1424(m)	1425(m)	1423 (m) P	1426DO	1422(21) Dimer	D
						1421 (23) Dimer	
						1416 (23) Dimer	
						!402 (3) Dimer	
1375 (w)						1390 (21) Trimer D	OR
1360 (w)						1385 (17) Trimer A	OR
						1371 (22) Trimer D	
						1368 (19) Trimer A	

[a] Experimental intensities are given in parentheses. Abbreviations: vs = very strong; s = strong; m = medium; w = weak; vw = very weak. [b] Frequencies assigned to the C_{60} monomer are given in bold. [c] Assignments to a certain polymeric phase are given according to refs 10 and 42. Abbreviations: D = dimer; P = polymer; O = orthorhombic; T = tetragonal; R = rhombohedral. [d] Calculated intensities (km mol^{-1}) are given in parentheses. [e] Assignments: M = monomer; D = Dimer; O = orthorhombic; T = tetragonal; R = rhombohedral.

TABLE 5: IR Frequencies Observed in the 1300−1000 cm^{-1} Range (in cm^{-1}) of the Polymerized C_{60} Film and Harmonic Frequencies Calculated at the B3LYP/3-21G Level of Theory for the C_{60} Monomer, Dimer, and Trimers

observed							
this work	ref 18	ref 4	ref 40	ref 42	ref 10	calculated	C_{60} phase
1273 (w)	1277 (w)		1270 (w)[a]		1260 O 1263 T	1271 (3) Dimer 1265 (6) Dimer	D
1233 (w)	1228 (m)	1229 (w)	1225 (w)[a]	1229 (m) P	1230 D 1228 O 1228 T	1230 (4) Dimer 1223 (9) Dimer 1212 (3) Dimer	D
1188 (w)			1188 (m)		1189 D	1180 (32) Dimer	D
1182 (w)	1183 (s)	1183 (w)		1183 (m) DP	1180 D 1183 O 1184 D	1175 (12) Monomer 1175 (8) Dimer	MD

[a] See footnotes in Table 4.

TABLE 6: IR Frequencies Observed in the 1000−600 cm^{-1} Spectral Range (in cm^{-1}) of Polymerized C_{60} Film, and Harmonic Frequencies Calculated at the B3LYP/3-21G Level of Theory of C_{60} Monomer, Dimer and Trimers[a]

observed							
this work	ref 18	ref 4	ref 40	ref 42	ref 10	calculated	C_{60} phase
797 (m)	793 (s)	796 (m)	796 (s)	796 (s) DP	796 D	792 (9) Dimer	D
770 (w)	769 (w)	769 (w)	770 (s)	769 (m) P	770 D 778 O 768 T	787 (23) Dimer	DT
761 (w)	760 (w)	761 (w)	752 (s)	761 (m) DP	759 O 764 R	764 Trimer A 751 Trimer D	OR
743 (w)	745 (w)	743 (w)	746 (m)	743 (m) DP	742 D 741 T 743 R	745 Dimer	DRT
732 (vw)				732 (m) P	732 D 730 O/T	737 Trimer A 735 Trimer D	OT
727 (vw)		727 (w)		726 (s) P	728 D/O	725 Trimer A	OT
720 (vw)				720 (w)	718 R 716 O/T	721 Trimer D	R
711 (w)	712 (m)		710 (m)	707 (m) DP	711 D/O/T	719 (25) Dimer	D
707 (w)		709 (w)	706 (m)	707 (m) DP	709 R 708 O 706 D	706 (37) Dimer	D
701 (w)	701 (w)			702 (m) P		700 Trimer A	P
622 (vw)				624 (w) D 623 (m) P		630 Trimer A 627 Trimer D	P
617 (w)	618 (w)	616 (w)		618 (m) P 619 (m) D		620 Trimer A 615 Trimer A	P
612 (w)	612 (m)		612 (s)	612 (m) P	613 D 612 O	609 (16) Dimer	DO
607 (vw)	607 (m)			607 (w) P	608 R 605 T	605 Trimer A	TR

[a] See footnotes in Table 4.

the bands' frequencies with respect to the dimer band at 1460 cm^{-1}, and this agrees with the experimental data.

In the 1400−1350 cm^{-1} range, the calculations predict several weak bands of Trimers A, B, and C that we attribute to the weak experimental bands at 1375 and 1360 cm^{-1}. No dimer bands are observed in the 1350−1300 cm^{-1} range, most probably because of their very low intensities.

4.3.2. 1300−1000 cm^{-1}. Results obtained for this region are presented in Table 5. After 27 h of UV irradiation, a new weak band with a maximum at the frequency 1188 cm^{-1} corresponding to the dimer appears near the decreasing monomer band of 1182 cm^{-1}.[10,40] The calculations predict a band for the monomer and the dimer at 1175 cm^{-1} and another dimer band at 1180 cm^{-1}. The upshift of the 1188 cm^{-1} dimer band by 6 cm^{-1} in comparison with the 1182 cm^{-1} band of the monomer agrees with the theoretically predicted shift of 5 cm^{-1}. Moreover, virtually coincidental with the monomer band, a new band appears, which was previously observed for the photopolymer.[4,18] This band corresponds to the O polymer and the dimer.[10] Calculations predict almost identical frequencies at 1175/1174 cm^{-1} for the monomer, the dimer, and Trimer D. The weak bands observed previously for the photopolymer[4,18] appear at the frequencies 1273 and 1233 cm^{-1}. These bands coincide with the calculated dimer frequencies at 1271, 1265 and 1230, 1223 cm^{-1}. However, according to the calculations, in this region, some weak bands of polymeric phases may also be present, as can be found by examining the trimer frequencies shown in Table 5. Therefore, at this point, a definite assignment of the bands at 1273 and 1233 cm^{-1} is not possible.

4.3.3. 1000−600 cm^{-1}. The most intensive band in this region is observed at 797 cm^{-1}, and it matches well the frequency of 792 cm^{-1} predicted for the C_{60} dimer (Table 6). This band was also observed for C_{60} polymerized by other methods.[4,10,18,40] Two more bands in this region are observed at 770 and 761 cm^{-1}. The calculations predict the presence of a band of the dimer at 787 cm^{-1} and several bands of Trimer A and Trimer D between 770 and 745 cm^{-1}, as shown in Table 6. On the basis of these data, we assigned the experimental band at 770 cm^{-1} to the dimer and the band at 761 cm^{-1} to the O and/or T polymer. The band at the frequency 743 cm^{-1} was observed earlier for the photopolymer,[4] and, according to refs 10 and 40, it can correspond to either the dimer and/or T/R polymers. The weak

TABLE 7: IR Frequencies Observed in the 600−450 cm^{-1} Spectral Range (in cm^{-1}) of Polymerized C_{60} Film, and Harmonic Frequencies Calculated at the B3LYP/3-21G Level of Theory for C_{60} Monomer, Dimer and Trimers[a]

observed							
this work	ref 18	ref 4	ref 40	ref 42	ref 10	calculated	C_{60} phase
576 (m)	576 (s)				576 (O)	584 (7) Dimer 581 (12) Monomer	M
574 (m)			574 (s)	574 (s) P	574 D	576 (3) Dimer	D
567 (vw)	568 (m)	569 (m)		567 (s) PD	565 T	569 Trimer D	T
560 (w)	561 (m)		560 (s)	561 (m) P	561 D	563 (8) Dimer	D
552 (w)	552 (m)	550 (m)	550 (s)	552 (s) P 551 (m) D	554 O 550 DR	554 (19) Dimer	D
547 (vw)			545 (m)	547 (m) P	546 DT	550 (2) Dimer	DT
542 (vw)	542 (s)				543 O	546 Trimer	O
536 (vw)	540 (m) 537 (w)			537 (m) P	532 T	539 Trimer	T
526 (s)	526 (s)	526 (s)	527 (vs)	526 (s) DP	526 DO 524 R	526 Monomer 525 Dimer	DO
485 (vw)	482 (m)	484 (m)		487 (w) P	486 D	490 Dimer	DT
477 (vw)	479 (w)		479 (s)	476 (m) D	485 T	475 Dimer 475 Trimer	D
467 (vw)	468 (m)			470 (w) P		470 Trimer	T

[a] See footnotes in Table 4.

band at the frequency 732 cm^{-1} was not observed earlier for the photopolymer. Here, we assign it to the O or T polymer.

The band at 711 cm^{-1} was observed earlier for the photopolymer.[18] It corresponds to the dimer. The corresponding calculated frequency is 719 cm^{-1}. The band at 707 cm^{-1} is also assigned to the dimer (the calculated frequency is 706 cm^{-1}), and it was observed previously for the C_{60} films obtained by other methods.[4,40,42] Although the band at 701 cm^{-1} was observed earlier for the photopolymer,[18] here we attribute it to the O polymer on the basis of the frequencies predicted for Trimer D.

Three weak bands are observed at 622, 617, and 612 cm^{-1}. The band at 612 cm^{-1} was earlier observed for the dimer phase[40] and agrees well with the frequency predicted for the dimer at 609 cm^{-1}. The bands at 622 and 617 cm^{-1} are attributed to the polymer phases O and T since they are absent in the IR spectrum of the dimer phase.[40] For Trimers A and D, the calculations predict intensive bands at 627, 626, 620, and 619 cm^{-1}. As for the polymers prepared with the solution-based method,[42] these bands or bands within their close proximity have been observed in the spectra of both fullerene dimers and polymers. The weak band at 607 cm^{-1} appeared in the film spectra only after 27 h of irradiation (such a band was observed earlier for the photopolymer[18]) and likely corresponds to the T and/or R polymer[10] since the corresponding Trimer A band is predicted at 605 cm^{-1}.

4.3.4. 600−450 cm^{-1}. The frequencies observed and predicted for this spectral region are summarized in Table 7. After irradiation, a new band appeared at 574 cm^{-1} near the monomer band at 576 cm^{-1}. The intensity of this latter band after irradiation decreased. The new band is attributed to the dimer.[10,40] Calculations also predict a downshift of the dimer 576 cm^{-1} band with respect to the corresponding monomer band at 584 cm^{-1}. The band at 552 cm^{-1} was previously observed for the photopolymer.[4,18] We also assign it to the dimer since its calculated frequency is 554 cm^{-1}. Some small contributions of O and R polymers[10] can also appear near this band.

The band at 560 cm^{-1} observed earlier for the photopolymer[18] may be assigned to the dimer.[10,40] A weak band at 567 cm^{-1} was also observed for the photopolymer.[18] According to refs 10 and 40, its appearance is due to the O polymer, and it matches the calculated frequency for Trimer D.

A weak band at 547 cm^{-1} was not previously revealed in the photopolymer spectrum. The band can be due to the dimer and/or the T polymer.[10] A weak band appearing at 542 cm^{-1} after long-term irradiation was previously observed for the photopolymer,[18] and, according to ref 10 and the predicted frequency of Trimer D at 546 cm^{-1}, it may be attributed to the O polymer.

The intensity of the strongest band of the monomer at 526 cm^{-1} decreases with the rise of the dose of the UV irradiation, but, compared with other monomer lines, the decrease rate of the band is slower. This results from the appearance of a new band at this frequency, corresponding to the dimer.[40] Also, a contribution from the O polymer should not be excluded at this frequency.[10] The neighboring (weak) band at 536 cm^{-1} was previously observed for the photopolymer[18] and, most probably, corresponds to the T polymer.[10,41]

In the 400−500 cm^{-1} region of the spectrum, three weak bands appear in the spectrum. They were also observed earlier in the photopolymer.[18] The band at 485 cm^{-1} was observed earlier in the photopolymer.[4,18] According to ref 10, this band can be assigned to the dimer and/or the T polymer. The band at 477 cm^{-1} was previously observed in the dimer spectra[40,42] but was not detected for the polymers produced by the HPHT method.[10] The band at 469 cm^{-1} was not previously observed either for the dimer[40,42] or for the T polymer.[41] However, this band was observed for other polymers[42] and can be due to the O or R polymer.

5. Conclusions

On the basis of the analysis of the IR absorption spectra (Tables 4−7), we can conclude that, in our photopolymerized C_{60} films, all standard polymeric phases are formed. Most of the observed bands are attributed to the dimer and to the O phase. A small amount of monomers estimated for less than 5% was also observed. Some of the T and R polymer phases were also found. A detailed analysis of the IR spectra of the photopolymerized C_{60} films allowed us to assign most of the observed bands. On the basis of this assignment, we determined spectral bands that can be used to identify certain polymeric phases in the C_{60} films. The bands at 1458, 1273, 1233, 797, and 770 cm^{-1} can be used to identify the dimer phase because they do not overlap with either monomer or trimer bands. The bands at 1375, 1360, 732, 727, 720, and 467 cm^{-1} can be used to identify the O, T, or R polymeric phase because they do not overlap with any of the monomer or dimer bands.

We found that the DFT frequency calculations performed with the B3LYP functional are capable of reproducing experimental vibrations, even if a relatively small basis set (3-21G) is employed. After applying two scaling factors (0.98 and 1.04 for higher and lower frequencies, respectively), the difference between the calculated and the observed frequencies does not exceed 10 cm^{-1}.

Acknowledgment. This work was supported by the Science Technology Center of Ukraine (Project No. 1934) and by the Ministry of Education and Science of Ukraine (Grant M228-2004).

References and Notes

(1) Blank, V. D.; Buga, S. G.; Serebryanaya, N. R.; Denisov, V. N.; Dubitsky, G. A.; Ivlev, A. N.; Mavrin, B. N.; Popov, M. Yu. *Phys. Lett. A* **1995**, *205*, 1995.

(2) Brazhkin, V. V.; Lyapin, A. G.; Popova, S. V.; Klyuev, Yu. A.; Naletov, A. M. *J. Appl. Phys.* **1998**, *84*, 219.

(3) Makarova, T. L.; Sundqvist, B.; Hohne, R.; Esquinazl, P.; Kopelevich, Y.; Scharff, P.; Davydov, V. A.; Kashevarova, L. S.; Rakhmanina, A. V. *Nature* **2001**, *413*, 716.

(4) Rao, A. M.; Zhou, P.; Wang, K.-A.; Hager, G. T.; Holden, J. M.; Wang, Y.; Lee, W. T.; Bi, X. X.; Eklund, P. C.; Cornett, D. S.; Duncan, M. A.; Amster, I. J. *Science* **1993**, *259*, 955.

(5) Iwasa, Y.; Arima, T.; Fleming, R. M.; Siegrist, T.; Zhou, O.; Haddon, R. C.; Rothberg, L. J.; Lyons, K. B.; Carter, H. L., Jr.; Hebard, A. F.; Tycko, R.; Dabbagh, G.; Krajewski, J. J.; Thomas, G. A.; Yagi, T. *Science* **1994**, *264*, 1570.

(6) Bashkin, I. O.; Rashchupkin, V. I.; Kobelev, N. P.; Moravsky, A. P.; Soifer, Y. M.; Ponyatovsky, E. G. *JETP Lett.* **1994**, *59*, 258.

(7) Bashkin, I. O.; Rashchupkin, V. I.; Gurov, A. F.; Moravsky, A. P.; Rybchenko, O. G.; Kobelev, N. P.; Soifer, Y. M.; Ponyatovsky, E. G. *J. Phys.: Condens. Matter* **1994**, *6*, 7491.

(8) Núñez-Regueiro, M.; Marques, L.; Hodeau, J.-L.; Béthoux, O.; Perroux, M. *Phys. Rev. Lett.* **1995**, *74*, 278.

(9) Oszlanyi, G.; Forro, L. *Solid State Commun.* **1995**, *95*, 265.

(10) Davydov, V. A.; Kashevarova, L. S.; Rakhmanina, A. V.; Senyavin, V. M.; Céolin, R.; Szwarc, H.; Allouchi, H.; Agafonov, V. *Phys. Rev. B* **2000**, *61*, 11936.

(11) Moret, R.; Launois, P.; Wagberg, T.; Sundqvist, B. *Eur. Phys. J. B* **2000**, *15*, 253.

(12) Okada, S.; Saito, S. *Phys. Rev. B* **1999**, *55*, 1930.

(13) Suzuki, M.; Iida, T.; Nasu, K. *Phys. Rev. B* **2000**, *61*, 2188.

(14) Sakai, M.; Ichida, M.; Nakamura. A. *Chem. Phys. Lett.* **2001**, *335*, 559.

(15) Long, J. P.; Chase, S. J.; Kabler, M. N. *Chem. Phys. Lett.* **2001**, *347*, 29.

(16) Wang, Y.; Holden, J. M.; Rao, A. M.; Eklund, P. C.; Venkateswaran, U. D.; Eastwood, D.; Lidberg, R. L.; Dresselhaus, G.; Dresselhaus, M. S. *Phys. Rev. B* **1995**, *51*, 4547.

(17) Burger, B.; Winter, J.; Kuzmany, H.; *Z. Phys. B* **1996**, *101*, 227.

(18) Onoe, J.; Nakao, A.; Takeuchi, K. *Phys. Rev. B* **1997**, *55*, 10051.

(19) Rao, A. M.; Eklund, P. C.; Hodeau, J.-L.; Marques, L.; Nunez-Regueiro, M. *Phys. Rev. B* **1997**, *55*, 4766.

(20) Matsuishi, K.; Ohno, T.; Yashida, N.; Nakanishi, N.; Onari, S.; Arai, T. *J. Phys. Chem. Solids* **1997**, *58*, 1747.

(21) Wagberg, T.; Persson, P. A.; Sundqvist, B.; Jacobsson, P. *Appl. Phys. A: Mater. Sci. Process.* **1997**, *64*, 223.

(22) Rao, A. M.; Eklund, P. C.; Venkateswaran, U. D.; Tucker, J.; Dunkan, M. A.; Bendele, G. M.; Stephens, P. W.; Hodeau, J. L.; Marques, L.; Núñez-Regueiro, M.; Bashkin, I. O.; Ponyatovsky, E. G.; Morovsky, A. P. *Appl. Phys. A: Mater. Sci. Process.* **1997**, *64*, 231.

(23) Wagberg, T.; Jacobsson, P.; Sundqvist, B. *Phys. Rev. B* **1999**, *60*, 4535.

(24) Makarova, T. L.; Sakharov, V. I.; Serenkov, I. T.; Vul', A. Ya. *Phys. Solid State* **1999**, *41*, 497.

(25) Karachevtsev, V. A.; Vovk, O. M.; Plokhotnichenko, A. M.; Peschanskii, A. V. *Structural and Electronic Properties of Molecular Nanostructures*, AIP Conference Proceedings 633, XVI International Winterschool on Electronic Properties of Novel Materials, Kirchberg, Tirol, Austria, March 2−9, 2002; American Institute of Physics: Melville, NY, 2002; pp 17−20.

(26) Matsuzawa, N.; Ata, M.; Dixon, D. A.; Fitzgerald, G. *J. Phys. Chem.* **1994**, *98*, 2555.

(27) Adams, G. B.; Page, J. B.; Sankey, O. F.; O'Keeffe, M. *Phys. Rev. B* **1994**, *50*, 17471.

(28) Kurti, J.; Nemeth, K. *Chem. Phys. Lett.* **1996**, *256*, 119.

(29) Strout, D. L.; Murry, R. L.; Xu, C.; Eckhoff, W. C.; Odam, G. K.; Scuseria, G. E. *Chem. Phys. Lett.* **1993**, *214*, 576.

(30) Scuseria, G. E. *Chem. Phys. Lett.* **1996**, *257*, 583.

(31) Osawa, S.; Sakai, M.; Osawa, E. *J. Phys. Chem. A* **1997**, *101*, 1378.

(32) Porezag, D.; Pederson, M. R.; Frauenheim, Th.; Köhler, Th. *Phys. Rev. B* **1995**, *52*, 14963.

(33) Lee, K. H.; Eun, H. M.; Park, S. S.; Suh, Y. S.; Jung, K.-W.; Lee, S. M.; Lee, Y. H.; Osawa, E. *J. Phys. Chem. B* **2000**, *104*, 7038.

(34) Kunitake, M.; Uemura, S.; Ito, O.; Fujiwara, K.; Murata, Y.; Komatsu, K. *Angew. Chem., Int. Ed.* **2002**, *41*, 969.

(35) Becke, A. D. *Phys. Rev. B* **1988**, *38*, 3098.

(36) Lee, C.; Yang, W.; Parr, R. G. *Phys. Rev. B* **1988**, *37*, 785.

(37) Vosko, S. H.; Wilk, L.; Nusair, M. *Can. J. Phys.* **1980**, *58*, 1200.

(38) Frisch, M. J.; Trucks, G. W.; Schlegel, H. B.; Scuseria, G. E.; Robb, M. A.; Cheeseman, J. R.; Montgomery, J. A., Jr.; Vreven, T.; Kudin, K. N.; Burant, J. C.; Millam, J. M.; Iyengar, S. S.; Tomasi, J.; Barone, V.; Mennucci, B.; Cossi, M.; Scalmani, G.; Rega, N.; Petersson, G. A.; Nakatsuji, H.; Hada, M.; Ehara, M.; Toyota, K.; Fukuda, R.; Hasegawa, J.; Ishida, M.; Nakajima, T.; Honda, Y.; Kitao, O.; Nakai, H.; Klene, M.; Li, X.; Knox, J. E.; Hratchian, H. P.; Cross, J. B.; Bakken, V.; Adamo, C.; Jaramillo, J.; Gomperts, R.; Stratmann, R. E.; Yazyev, O.; Austin, A. J.; Cammi, R.; Pomelli, C.; Ochterski, J. W.; Ayala, P. Y.; Morokuma, K.; Voth, G. A.; Salvador, P.; Dannenberg, J. J.; Zakrzewski, V. G.; Dapprich, S.; Daniels, A. D.; Strain, M. C.; Farkas, O.; Malick, D. K.; Rabuck, A. D.; Raghavachari, K.; Foresman, J. B.; Ortiz, J. V.; Cui, Q.; Baboul, A. G.; Clifford, S.; Cioslowski, J.; Stefanov, B. B.; Liu, G.; Liashenko, A.; Piskorz, P.; Komaromi, I.; Martin, R. L.; Fox, D. J.; Keith, T.; Al-Laham, M. A.; Peng, C. Y.; Nanayakkara, A.; Challacombe, M.; Gill, P. M. W.; Johnson, B.; Chen, W.; Wong, M. W.; Gonzalez, C.; Pople, J. A. *Gaussian 03*, revision B.05; Gaussian, Inc.: Pittsburgh, PA, 2003.

(39) Karachevtsev, V. A.; Mateichenko, P. V.; Nedbailo, N. Yu.; Peschanskii, A. V.; Plokhotnichenko, A. M.; Vovk, O. M.; Zubarev, E. N.; Rao, A. M. *Carbon*, submitted for publication, 2006.

(40) Komatsu, K.; Wang, G. W.; Murata, Y.; Tanaka, T.; Fujiwara, K.; Yamamoto, K.; Saunders, M. *J. Org. Chem.* **1998**, *63*, 9358.

(41) Zhu, Z.-T.; Musfeldt, J. L.; Kamaras, K.; Davydov, V. A.; Kashevarova, L. S.; Rakhmanina, A. V. *Phys. Rev. B* **2002**, *65*, 108543.

(42) Ma, B.; Milton, A.; Sun, Y. *Chem. Phys. Lett.* **1998**, *288*, 854.